Dual Frequency Comb Laser Absorption Spectroscopy in a 16 MW Gas Turbine Exhaust

P.J. Schroeder, R.J. Wright, S. Coburn, B. Sodergren,

Precision Laser Diagnostics Laboratory, Department of Mechanical Engineering, University of Colorado Boulder, Boulder, CO 80309, USA

K.C. Cossel, S. Droste, G.W. Truong, E. Baumann, F.R. Giorgetta, I. Coddington, N.R. Newbury

National Institute of Standards and Technology, Boulder, CO 80305, USA

G.B. Rieker

Precision Laser Diagnostics Laboratory, Department of Mechanical Engineering, University of Colorado Boulder, Boulder, CO 80309, USA

Abstract

We demonstrate the first frequency comb laser absorption spectroscopy in an industrial environment. Recent advancements in robust frequency comb design enable installation of the sensor in an operating power plant, where we simultaneously measured temperature, H_2O and CO_2 concentration in the exhaust of a 16MW stationary gas turbine. The frequency comb laser spectrometer probed 16,000 individual wavelengths of light spaced by 0.007cm^{-1} (0.0014nm) near 1440nm, spanning 279 absorption features of H_2O and 43 features of CO_2. Fits to the measured absorption spectra yield simultaneous temperature, H_2O and CO_2 concentrations with between 10 and 60 second time resolution. Measurements over a 5 hour period tracked variations in the exhaust consistent with various changes to the gas turbine operation. Much larger wavelength ranges (200+ nm) and different time resolutions are possible depending on the desired precision by changing various settings on the same spectrometer. Overall, this work demonstrates the potential for frequency comb laser absorption spectroscopy in industrial combustion environments.

Keywords: frequency comb, combustion, absorption spectroscopy, sensor, gas turbine

1. Introduction

Mode-locked frequency combs are a special class of laser that simultaneously emit hundreds of thousands of perfectly spaced "comb teeth" – narrow-linewidth, phase-coherent wavelengths of light that are all separated by the pulse repetition frequency of the laser (10s of MHz to GHz)[1-2]. Though they were initially developed for time and frequency metrology, researchers quickly recognized that frequency combs could be a useful tool for broadband laser absorption spectroscopy, where many absorption features from several molecules could be measured with one laser[3]. To accurately resolve the absorption spectra of small molecules with ~GHz absorption linewidths at atmospheric pressure, it is desirable to use frequency comb sources with a comb tooth spacing on the order of a few hundred MHz – a few picometers in wavelength space. However, it is difficult to resolve these closely-spaced comb teeth and simultaneously measure a large wavelength range using traditional broadband detection systems. Dual frequency comb spectroscopy (DCS) addresses this issue by spectrally resolving each comb tooth through interference with a second frequency comb [4–6]. The second frequency comb is phase-locked to the first frequency comb, but with a slightly different repetition rate (and hence tooth spacing). After passing through the sample of interest, the two combs interfere on a single high-speed photodetector and each pair of nearest comb teeth gives rise to a unique heterodyne beat frequency. The strength of each beat signal is proportional to the electric field amplitudes of the two contributing comb teeth. If absorption occurs on either of the teeth, the beat signal is reduced. In this way, absorption can be measured on each individual comb tooth across a very broad wavelength range using a single photodetector (see Figure 1).

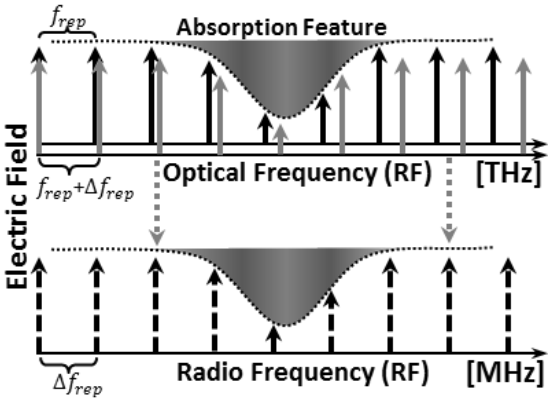

Figure 1-Concept of DCS spectroscopy. Two combs are stabilized so each nearest pair of comb teeth has a slightly different frequency offset, leading to a unique RF beat signal on the detector.

We recently demonstrated that comb-tooth-resolved DCS is possible in practical environments, despite decohering effects induced by turbulence [7-8]. These prior experiments were performed with a laboratory-based dual-comb spectrometer built around ring cavity laser oscillators that utilize nonlinear polarization rotation mode-locking, and which were phase-locked to two cavity-stabilized, narrow-linewidth, single-frequency lasers [9]. A hydrogen maser (ultra-stable frequency reference) provided the timebase for all electronics. The mode-locking was highly sensitive to vibration, temperature, and humidity changes, and the combs where incompatible with field operation. Phase-locking the combs to cavity-stabilized lasers and referencing them to the hydrogen maser provided a high degree of frequency accuracy and stability (Hz linewidth comb teeth and knowledge of the absolute comb tooth frequency to <1kHz), but came with high cost and complexity.

Here we present the first demonstration of a mobile dual-comb spectrometer for measurements in an industrial environment. The mobile spectrometer takes advantage of several recent advancements in environmentally robust frequency comb lasers [10-11] to untether the dual-comb system from the laboratory. These frequency combs demonstrate stable mode-locking despite temperature changes of more than 10°C, relative humidity variations from 30-100%, and vibrations up to 1.3g max acceleration[10]. The spectrometer configuration also eliminates the need for both the cavity-stabilized lasers and the hydrogen maser for phase locking and wavelength referencing.

We characterize the exhaust of a 16MW stationary gas turbine in the University of Colorado cogeneration facility by recording absorption spectra composed of 16,000 comb teeth spanning 1435.5nm to 1445.1nm with 1.4picometer wavelength spacing. The actual instrument resolution is better than 1picometer because the linewidth of each tooth is approximately 2kHz, and the frequencies are conservatively known to better than 10MHz (see below for details). Spectra containing 279 absorption features of H_2O and 43 features of CO_2 are acquired at 12.4kHz, and averaged to achieve high signal-to-noise ratio (for between 10 and 60 seconds to achieve 5500 absorbance SNR here). They are simultaneously fit with HITRAN2012 based absorption models to extract temperature and species

concentrations. H_2O and CO_2 concentration levels are consistent with expectations based on turbine operating parameters. Temperature and concentration trends follow operational variations of the gas turbine and periodic operation of an auxiliary burner located in the duct upstream of the beam location.

These measurements demonstrate the feasibility of DCS for combustion environments. The kHz acquisition rates of the spectrometer are faster than turbulence-induced beam fluctuations in these environments, which enables undistorted full resolution spectra. This is not possible with high resolution Fourier transform spectrometers (FTS/FTIR), which are several orders of magnitude slower. With the current system, any species with absorption features in the 1 to 2.2 μm wavelength region can be probed simultaneously [12]. Future systems will further enhance the signal-to-noise ratio of dual comb spectrometry for short averaging times. Systems operating in the mid-infrared where stronger absorption features of even more molecules are located, are fast evolving [13].

2. Mobile Dual Frequency Comb Spectrometer

At the core of the mobile spectrometer are two frequency comb lasers based on a recent linear-cavity frequency comb design [10-11]. The design has all polarization-maintaining optical fiber components, and mode-locking is achieved with a semiconductor saturable absorber. Mode-locking in the laser is automatic and robust against environmental changes, and the fiber design is compact and portable. The frequency combs produce ~300mW of power from 1 to 2+μm. Each comb occupies a 20x20x2.5cm aluminum box that is temperature controlled with thermoelectric coolers. Pump lasers and control electronics are external to this box.

The two frequency combs must be phase-locked to one another and the wavelengths of the comb teeth must be referenced to a known wavelength in order to perform accurate heterodyne spectroscopy. The mobile implementation achieves phase-locking and wavelength-referencing using portable

components which achieve accuracy and stability appropriate for atmospheric pressure absorption spectroscopy measurements.

The frequency of each comb tooth is given by: $f_n = f_{ceo} + n * f_{rep}$ where f_n is the optical frequency of the nth comb tooth, f_{ceo} is the carrier-envelope-offset frequency, and f_{rep} is the repetition rate of the comb. Thus the comb has two degrees of freedom that must be controlled to achieve fully stabilized operation. The f_{ceo} is detected through a standard f-2f interferometry technique that compares a frequency-doubled comb tooth from the 2μm region to a tooth at 1μm [1,2,10,11]. Once detected, f_{ceo} can be phase locked to a reference oscillator through feedback to the comb oscillator pump power.

The phase-lock between the combs and control of f_{rep} is established by phase-locking one tooth near 1560nm from each comb to a narrow linewidth reference laser (2kHz linewidth, RIO Planex RIO0195-3-01-3). The comb structure is modulated through feedback to a piezoelectric stack that stretches the laser cavity. The particular tooth from each comb that is used for the lock is chosen judiciously (similar to the method outlined in [14]) for multi-heterodyne detection between the two combs. The accuracy and stability of the frequency locks depends on the radiofrequency oscillator that is used to reference the timebase of the electronics. For the implementations described in [6–9,14], the reference oscillator was a hydrogen maser with exceptional stability. Here, we use a compact ovenized quartz oscillator (Wenzel 501-09451) with stability better than 1ppm per day. In our wavelength range, this translates to MHz-level optical frequency stability. While lower than previous frequency comb implementations, this stability is comparable to a well-calibrated high-end FTIR and three orders of magnitude below the GHz absorption linewidths of typical atmospheric absorption features.

The narrow-linewidth reference laser itself drifts slowly by up to 100MHz (depending on environmental conditions) over a several hour period. This drift is transferred to the comb teeth. We measure the repetition rate of the frequency combs to mHz precision with a counter referenced to the quartz oscillator to measure the drift. This measurement, combined with the slow nature of the drift allows the proper wavelength scaling of each of our measured spectra with the MHz-level optical

frequency accuracy set by the quartz oscillator. The mobile dual-frequency comb spectrometer as installed at the power plant is shown in Figure **2**.

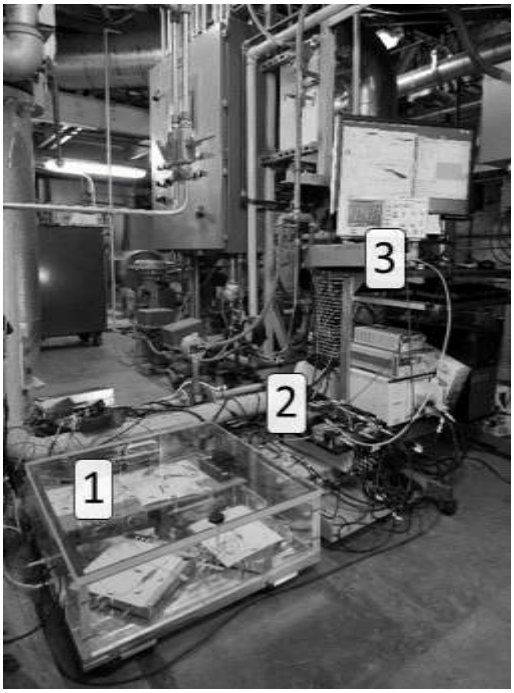

Figure 2- First industrial demonstration of a dual-frequency comb spectrometer. (1) Dual frequency combs (2) Reference laser, and (3) FPGA control electronics and data acquisition. The access port to the turbine exhaust is one floor above the spectrometer, and the spectral filters are out of the frame.

Other methods exist which allow correction for the frequency drift of comb teeth. These methods could also prove useful for mobile DCS[15,16].

The introduction of this spectrometer into combustion systems for the first time warrants a brief treatment of how the technique compares to other direct absorption techniques. The closest analog to this instrument is a Fourier Transform Spectrometer (FTS/FTIR). The resolution and sample time of an FTS are fundamentally determined by the length of its mechanically scanned Michelson interferometer arm. An FTS with comparable resolution to the comb spectrometer presented in this work would require a 1.5m scanning arm displacement, and thus is not robust and easily portable. More importantly, the spectral acquisition rate for such an instrument is several orders of magnitude slower than the comb spectrometer[17–19]. If individual spectra are not captured on timescales faster than the turbulence-

induced laser intensity fluctuations in a combustion system, the result is apodization (an effective loss of resolution and introduction of potential distortion). Supercontinuum sources and high-speed swept sources are capable of similar wavelength coverage and higher acquisition rates than dual-comb spectrometers, but are limited by some combination of unknown/broad laser linewidth (for swept sources), very difficult wavelength characterization (to establish an accurate, undistorted wavelength axis), and low spectral resolution (e.g. from the grating spectrometer or fiber dispersion methods used for detection of supercontinuum sources)[20–23]. TDLAS measurements achieve faster time resolution than the dual-comb technique and comparable spectral resolution, but cover only 1-2 absorption features of one species at low to moderate pressures. It is possible to multiplex diode lasers to measure multiple species at low to moderate pressures[24–26]. The comb spectrometer demonstrated here uses six pump diodes to generate 750,000 unique optical frequencies spanning from 1μm to 2+μm. Thus as the dual-comb technique becomes more accessible for industrial environments, we believe it fills a unique niche by providing flexible, broad spectral coverage, high resolution, and reasonably high acquisition rates.

3. Power Plant Facility

3.1. Stationary Gas Turbine Facility

The power plant at the University of Colorado Boulder is a cogeneration plant powered by two Mitsubishi MF111A/B 16MW natural gas turbines. The independent turbines use auxiliary steam injection into the combustor to lower peak temperatures and reduce NOx emissions. Combustor bypass air leads to overall lean operation (16% excess O_2). The exhaust passes through a heat exchanger to generate steam for turbine injection, additional power generation in a secondary steam turbine, and/or campus heating. Downstream of the turbine exit, there is a supplemental burner that is fired on demand to add energy to the exhaust for additional steam generation. Our measurement location was approximately 3.6m downstream of this burner, before the steam generation unit. The duct cross section at our measurement location was 4.6 x3.7m. See Figure **3** for an experimental schematic.

3.2. Optical Setup

The mobile dual-comb system rested on small inflated innertubes directly on the floor of the power plant, without further vibration isolation or control of the ambient temperature (see Figure **2**). Heavy machinery and large water pumps were continuously operating nearby during the course of the measurements and the ambient temperature varied from 12-22ºC. These severe external perturbations

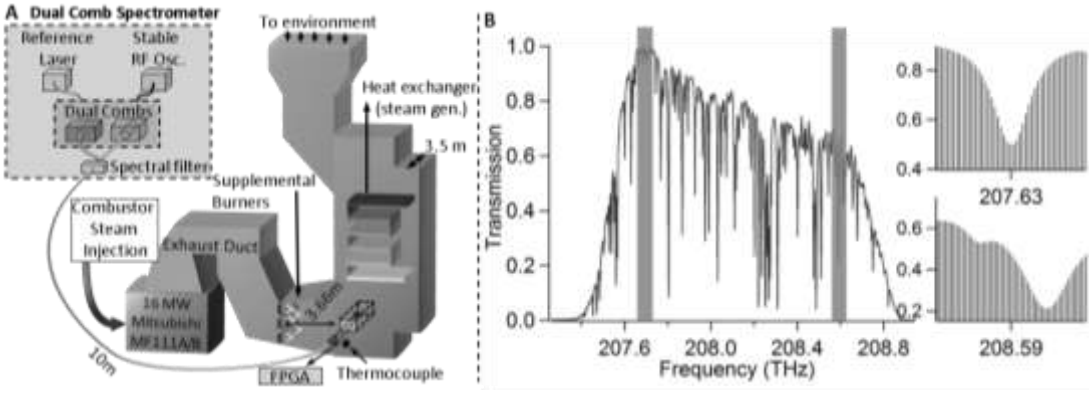

Figure 3-(A) Experimental schematic of the dual-comb spectrometer and gas turbine facility. (B) Example transmission spectrum with insets of two absorption features (vertical bars represent individual comb teeth).

did not affect the dual comb operation.

The light from the combs was combined, spectrally filtered to our region of interest (1435.5 to 1445.1nm), and sent through 10m of SMF-28 optical fiber to existing windows in the turbine exhaust duct, located one story above the spectrometer. The light was collimated into a 2.2mm diameter freespace beam with an off-axis parabolic mirror. The beam passed across the duct and was reflected back by a plane mirror for a roundtrip pathlength of 723cm. A 35mm plano-convex lens focused up to 175μW of return light onto a single photodetector (Thorlabs PDA10CF). A National Instruments field programmable gate array (National Instruments 7965 FPGA with 14-bit 5761 digitizer) sampled the detector at a rate of 200MHz, hardware-averaging 1000 interferograms (time-domain interference signals) before writing the data to disk.

In DCS, there is a tradeoff between the spectral bandwidth and acquisition rate of an individual spectrum. The spectral bandwidth is determined by the difference in the repetition rate of the two combs, which defines the spacing of the heterodyne beat frequencies in the detector signal. As the repetition rate difference is decreased, the heterodyne beat frequencies become closer together, and the beat signals from more comb tooth pairs can be detected between 0 Hz and $f_{rep}/2$ (after which the beat frequencies from subsequent comb tooth pairs begin aliasing). The acquisition time of a full resolution spectrum is equal to the difference of the repetition rates of the two combs, so as the repetition rate difference is decreased and the alias-free spectral bandwidth increases, the acquisition time also increases. This tradeoff is captured in the equation for the alias-free bandwidth, $f_{rep}^2/(2 * \Delta f_{rep})$. Here, we chose a relatively narrow spectral bandwidth (10nm) to increase the acquisition rate of an individual spectrum to 12.4kHz, thereby decreasing the averaging time to reach high SNR. A broader spectral range can be covered with the same system if a lower individual spectrum acquisition rate is acceptable.

4. Gas Turbine Exhaust Results

4.1. Absorption Spectra and Fitting

Figure **4** shows an example measured laser transmission spectrum from 207.46THz (1445.1nm) to 208.84THz (1435.5nm), after 60s of averaging. The absorbance noise for this condition was 0.5E-3, and the SNR for the strong water vapor absorption features was 5500. The comb tooth spacing is 200MHz (1.4picometers in this wavelength range). Temperature and species concentrations are inferred by simultaneously fitting the broad measured spectra with an absorbance model for each absorbing species, a polynomial function to account for broadband baseline variation, and a sine function to account for a distinct, stable etalon structure in the baseline induced by the existing 1cm-thick plane windows of the exhaust ports.

We fit the spectra in two distinct steps – a piecewise fit to correct the baseline, and then a bandwide fit to extract the temperature and species concentrations. First, the transmission spectrum is fit in smaller windows (~300GHz) with a 10^{th} order polynomial, a sine wave, and the absorption model with fixed temperature and pressure. Inclusion of the absorption model during baseline correction keeps the polynomial baseline from overfitting into the absorption feature wings. The resulting polynomial and sine functions are removed from the transmission data, leaving a normalized transmission spectrum. Next, we simulate a matrix of bandwide absorption models at a wide range of temperatures. A least squares routine fits the normalized spectrum with these absorption models, adjusting temperature and each species concentration until the bandwide fit error is minimized. Finally, we repeat the piecewise baseline correction and the bandwide fitting using newly estimated temperature and concentration values until convergence (normally 2-3 iterations). Note that incorporating improved high-temperature spectral parameters in the model should enable simultaneous fitting of pressure in the future. For the fit, we only retain HITRAN water and CO_2 lines exhibiting absorbance peaks resolvable above our noise floor of 0.5e-3. For these data, we fixed the pressure at a value of 645Torr, which was bracketed by local atmospheric pressure (about 635Torr) and the duct overpressure valve (set at 26Torr gauge pressure). Setting the fit pressure to these bounds resulted in a 2.2K rms difference in measured temperature.

Accurate absorption models that include the temperature and pressure dependence of the absorption features are vital to this process. Several databases catalogue molecular absorption feature strengths, widths, and locations, and are combined with a lineshape profile to create an absorption model. Here, we use a Voigt lineshape profile and absorption feature data from HITRAN2012 to generate an absorption spectrum for our measured region. HITRAN2012 was chosen because it contains many high-temperature absorption features from the HITEMP2010 database, in addition to newer experimental data [27]. Careful laboratory experiments using frequency combs to measure water vapor absorption spectra at known high temperature conditions show that HITRAN2012 is as good or better at predicting spectra up to 1300K than HITEMP2010 (Schroeder, in prep.). However, HITRAN2012 was developed without broadband high temperature experimental data, so the accuracy of absorption-feature strengths and air-broadening temperature-dependence at high temperatures still lags behind the accuracy of the corresponding data at room temperature. In addition, the database does not yet include the temperature dependence of pressure-shift and self-broadening coefficients. We are currently measuring and extracting these values for several thousand water features from 204THz to 215THz (Schroeder, in prep.). In the absence of these data, we use the following scaling relations for the self-broadening and pressure-shift coefficients, respectively [28]:

$$2\gamma_{self} = 2\gamma(T_o)\left(\frac{296}{T}\right)^{.5}, \qquad \delta_{air} = \delta_{air}(T_o)\left(\frac{296}{T}\right)^{1} \quad (1)$$

At the exhaust temperatures investigated, if the above scaling relationships are excluded, $2\gamma_{self}$ and δ_{air} are 36% and 59% larger than the unscaled values, respectively. To examine the sensitivity of the temperature and concentration retrievals to the scaling corrections, we refit a series of forty spectra without using the scaling corrections. This yielded a Root Mean Squared (RMS) difference between the retrieved temperature and concentration with and without the scaling of 23.9K, and 3.8e-3 for both H_2O

and CO_2. The same 40 data points were also refit perturbing every linestrength by the corresponding maximum HITRAN uncertainty, yielding an RMS temperature difference of 3.8K and 4.4e-3 in mole fraction for H_2O and CO_2. HITRAN line shape parameters were also perturbed to over-broaden and over-narrow each feature to the limits of the HITRAN line shape parameters, which resulted in an RMS temperature difference of 10.0K and 4.7e-3 in mole fraction for H_2O and CO_2.

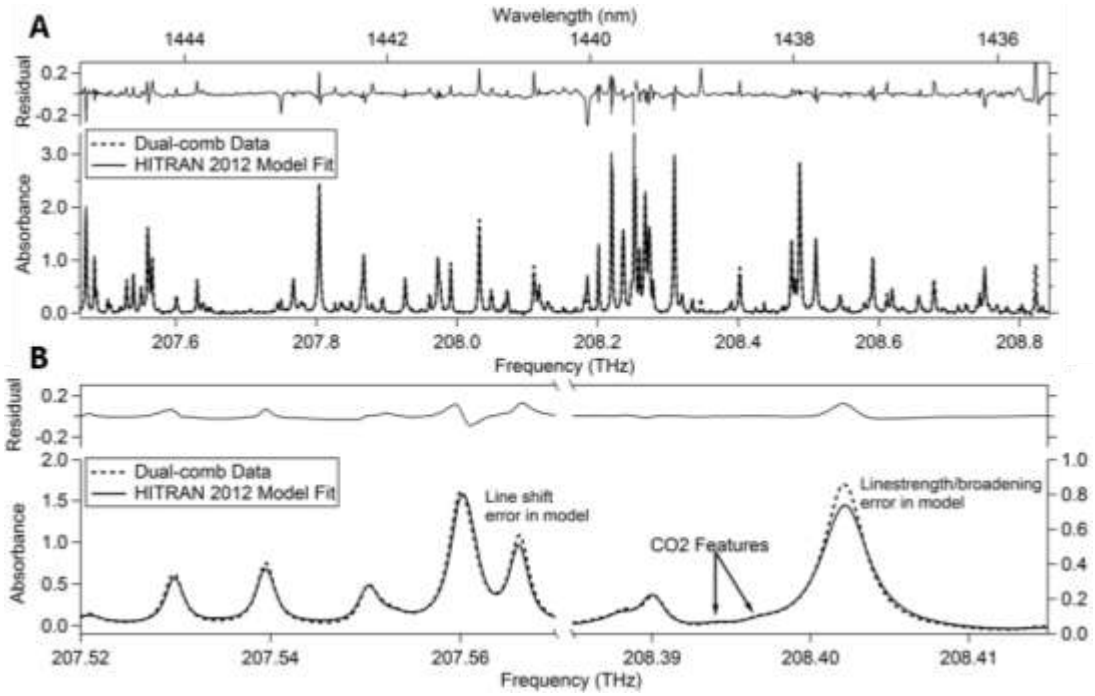

Figure 4-(A) Measured absorbance spectrum (60s average) with absorption model fit and residual. (B) Two example narrow spectral regions showing model fit and examples of common errors associated with the absorption database when used for high temperature environments. The right side of (B) shows two weak CO_2 features resolvable on the wings of strong neighboring water features. Note, absorbance is calculated to base e.

Figure 4A shows a typical spectrum, model fit, and the residual. We excluded residuals from the strongly saturated portions of features (absorbance greater than 2.75). Figure 4B shows two narrow regions of the fit. The extremely weak CO_2 absorption is resolvable and easily incorporated in the fit despite the strong neighboring water vapor absorption features. Water vapor overlap is typical for all the CO_2 features in our spectra. This illustrates one strength of the broadband capability of the spectrometer – the ability to simultaneously fit multiple interfering absorbing species. The decreased accuracy of many HITRAN2012 spectral parameters at high temperatures is apparent in Figure 4.

However, because the temperature and species concentrations are extracted from a bandwide fit to hundreds of features, sensitivity to error in individual lines is greatly reduced. Instead of using the ratio of absorbance from two features to determine temperature (as in most absorption thermometry techniques), we generate models at 2K temperature increments over the range of temperatures possible in the system. The least-squares fitting procedure finds the model spectrum that best represents the collected spectrum to determine temperature. Therefore, the spectrometer is mainly sensitive to overall systematic biases in the database parameters, instead of errors in linestrength or shape of individual absorption features.

4.2. Time-resolved Results

Figure **5** shows time-resolved temperature, H_2O and CO_2 concentrations during a 2.5 hour period that includes a temporary ignition of the supplementary burners and gas turbine shutdown. Each point represents a parameter extracted from a fit to a 60s average spectrum similar to Figure 4.

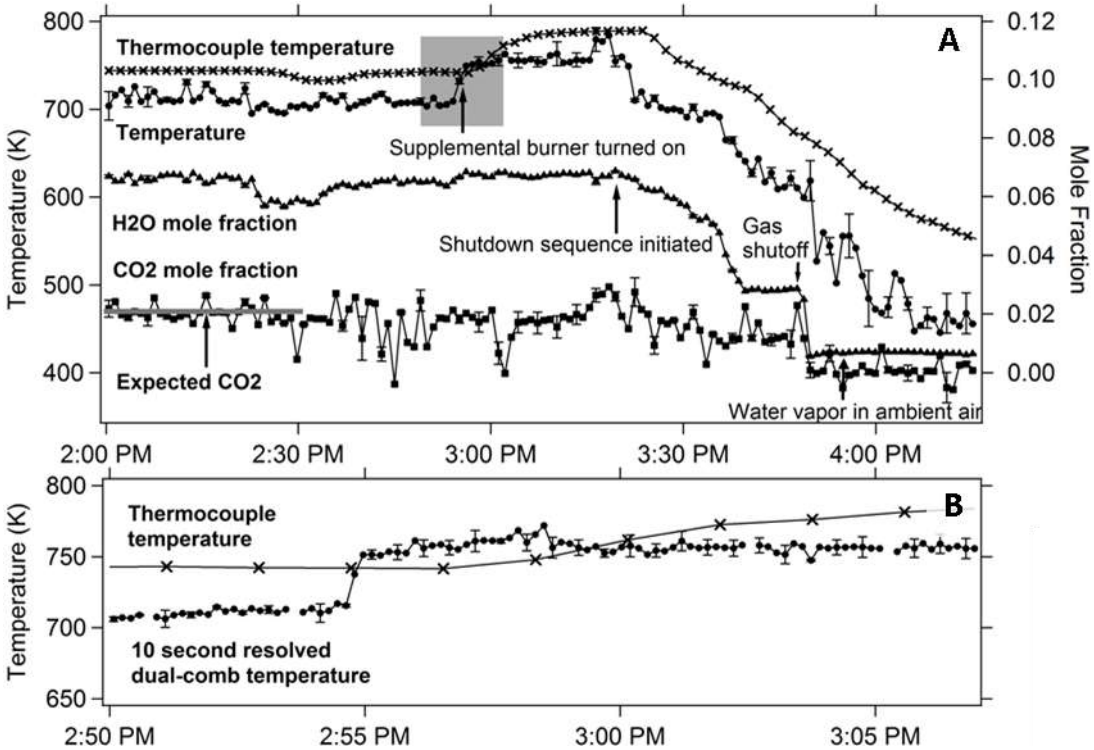

Figure 5-(A) Time-resolved measurements using the dual-comb spectrometer (60s averages). Temperature from nearest uncalibrated thermocouples to the measurement location (0.8m separation). The horizontal line at early times on the CO_2 trace represents the expected value based on the measured excess oxygen. (B) 10 second averaged temperature data during supplemental burner ignition.

The temperature results are compared to an uncalibrated, sheathed thermocouple approximately 0.8m below the laser beam and protruding an unknown distance into the exhaust flow. The sheathing improves the life but causes the measurement time lag. The plots show trend agreement between the frequency comb measurement and the thermocouple except for thermocouple lag during transients. We do not expect absolute temperature agreement because the thermocouple is uncalibrated and sampling a different region of the flow.

From 2:55P.M. to 3:21P.M. local time, the auxiliary exhaust duct burner was ignited, causing a rapid temperature increase immediately apparent with the frequency comb data but with some lag in the thermocouple data. The water mole fraction increases about 5% after the supplemental burner ignition. The larger uncertainty in the CO_2 measurements makes a similar increase less resolvable. Figure **5**B shows the measured temperature with 10s average data during the startup transient of the exhaust duct burner. Four points were removed from the 10s average data because of poor convergence of the spectral fit. At 3:21P.M. the auxiliary burner was shut off and the turbine shutdown sequence commenced. This lasted until the fuel flow to the turbine was completely shut off at 3:49P.M. The post processing fitting routine was seeded with an initial temperature guess of 700K +/- 10K (randomly generated) for the entire data run, so no a priori temperature profile information was required to seed the fitting routine and track the temperature trend.

Figure **5** also shows the frequency comb-measured water and CO_2 concentrations. The expected CO_2 concentration based on the measured excess O_2 is represented by a horizontal line during the stable period prior to 2:30PM. The mean laser-measured CO_2 concentration matches the expected concentration to within a relative error of 4.4%. The mean laser-measured H_2O concentration is higher than a simple stoichiometry calculation would suggest which is expected given ambient water vapor in the intake air and steam injection into the combustor. At 3:49PM, the natural gas flow to the turbine was shut off, and CO_2 concentrations fall to zero while the water concentration falls to the ambient level.

To estimate the statistical uncertainty of our measurements, we iterated the fit 15 times for each data point, using different guesses of the initial conditions, to obtain the standard deviation of the measured temperatures and concentrations at each step in the time series (represented by the uncertainty bars in Figure 5). Figure 5 shows every third uncertainty for clarity and the averages of all the deviations are : 1.2%, 1.0%, and 17.8% for temperature, H_2O, and CO_2, respectively. Note that the increased CO_2 deviation is due to the relatively weak CO_2 absorbance signal.

5. Summary

We demonstrate the first industrial application of a dual frequency comb spectrometer by measuring temperature, H_2O, and CO_2 concentration transients in the exhaust of a 16MW stationary natural gas turbine at the University of Colorado Boulder. The spectrometer was completely untethered from the laboratory, maintaining phase and mode lock for over six hours in a noisy industrial environment without the need for significant vibration isolation, ambient temperature control, cavity-stabilized reference lasers or an ultra-stable RF reference. Individual spectra measuring absorption on 16,000 distinct comb teeth were recorded at a rate of 12.4kHz and averaged for 10 or 60s. We simultaneously fit 279 H_2O and 43 CO_2 absorption features to obtain temperature and species concentrations. The measurements demonstrate the potential for a fieldable dual-comb spectrometer with a unique combination of acquisition speed, bandwidth, and resolution that have so far only been exploited by combs residing in a stable optics laboratory.

Acknowledgements

This work was funded by the National Science Foundation under Grant Number CBET 1454496 and by the Advanced Research Projects Agency-Energy (ARPA-E), U.S. Department of Energy, under Award Number DE-AR0000539. The views and opinions of authors expressed herein do not necessarily state or reflect those of the United States Government or any agency thereof. The authors would like to

thank Torrey Hayden, Amanda Makowiecki, David Pfotenhauer, and Jinyu Yang for their help during the measurement campaign. We also thank Ken Morse, Victor Ferreira, Jeffery Fisher, Steve Burke, and the control room staff at the CU power plant for help and access to their equipment.

References

[1] J. L. Hall, *Rev. Mod. Phys.*, vol. 78, no. 4, pp. 1279–1295, Nov. 2006.
[2] T. W. Hänsch, *Rev. Mod. Phys.*, vol. 78, no. 4, pp. 1297–1309, Nov. 2006.
[3] M. J. Thorpe, *Science*, vol. 311, no. 5767, pp. 1595–1599, Mar. 2006.
[4] F. Keilmann, C. Gohle, and R. Holzwarth, *Opt. Lett.*, vol. 29, no. 13, pp. 1542–1544, 2004.
[5] A. Schliesser, M. Brehm, F. Keilmann, and D. van der Weide, *Opt. Express*, vol. 13, no. 22, pp. 9029–9038, 2005.
[6] I. Coddington, W. Swann, and N. Newbury, *Phys. Rev. Lett.*, vol. 100, no. 1, Jan. 2008.
[7] G. B. Rieker, F. R. Giorgetta, W. C. Swann, J. Kofler, A. M. Zolot, L. C. Sinclair, E. Baumann, C. Cromer, G. Petron, C. Sweeney, P. P. Tans, I. Coddington, and N. R. Newbury, *Optica*, vol. 1, no. 5, p. 290, Nov. 2014.
[8] F. R. Giorgetta, G. B. Rieker, E. Baumann, W. C. Swann, L. C. Sinclair, J. Kofler, I. Coddington, and N. R. Newbury, *Phys. Rev. Lett.*, vol. 115, no. 10, p. 103901, 2015.
[9] A. M. Zolot, F. R. Giorgetta, E. Baumann, J. W. Nicholson, W. C. Swann, I. Coddington, and N. R. Newbury, *Opt. Lett.*, vol. 37, no. 4, p. 638, Feb. 2012.
[10] L. C. Sinclair, I. Coddington, W. C. Swann, G. B. Rieker, A. Hati, K. Iwakuni, and N. R. Newbury, *Opt. Express*, vol. 22, no. 6, p. 6996, Mar. 2014.
[11] L. C. Sinclair, J.-D. Deschênes, L. Sonderhouse, W. C. Swann, I. H. Khader, E. Baumann, N. R. Newbury, and I. Coddington, *Rev. Sci. Instrum.*, vol. 86, no. 8, p. 081301, Aug. 2015.
[12] S. Okubo, K. Iwakuni, H. Inaba, K. Hosaka, A. Onae, H. Sasada, and F.-L. Hong, *Appl. Phys. Express*, vol. 8, no. 8, p. 082402, 2015.
[13] F. Zhu, A. Bicer, R. Askar, J. Bounds, A. A. Kolomenskii, V. Kelessides, M. Amani, and H. A. Schuessler, *Laser Phys. Lett.*, vol. 12, no. 9, p. 095701, 2015.
[14] A. M. Zolot, F. R. Giorgetta, E. Baumann, W. C. Swann, I. Coddington, and N. R. Newbury, *J. Quant. Spectrosc. Radiat. Transf.*, vol. 118, pp. 26–39, Mar. 2013.
[15] J. Roy, J.-D. Deschênes, S. Potvin, and J. Genest, *Opt. Express*, vol. 20, no. 20, pp. 21932–21939, Sep. 2012.
[16] T. Ideguchi, A. Poisson, G. Guelachvili, N. Picqué, and T. W. Hänsch, *Nat. Commun.*, vol. 5, 2014.
[17] R. A. Toth, *J. Mol. Spectrosc.*, vol. 190, no. 2, pp. 379–396, Aug. 1998.
[18] P. S. Thomas, J.-P. Guerbois, G. F. Russell, and B. J. Briscoe, *J. Therm. Anal. Calorim.*, vol. 64, no. 2, pp. 501–508, May 2001.
[19] M. Birk and G. Wagner, "*J. Quant. Spectrosc. Radiat. Transf.*, vol. 113, no. 11, pp. 889–928, Jul. 2012.
[20] S. T. Sanders, *Appl. Phys. B*, vol. 75, no. 6–7, pp. 799–802, Nov. 2002.
[21] Y. Arita, R. Stevens, and P. Ewart, *Appl. Phys. B*, vol. 90, no. 2, pp. 205–211, 2008.
[22] S. A. Kovalenko, A. L. Dobryakov, J. Ruthmann, and N. P. Ernsting, *Phys. Rev. A*, vol. 59, no. 3, pp. 2369–2384, Mar. 1999.
[23] J. M. Langridge, T. Laurila, R. S. Watt, R. L. Jones, C. F. Kaminski, and J. Hult, *Opt. Express*, vol. 16, no. 14, p. 10178, Jul. 2008.
[24] R. M. Mihalcea, D. S. Baer, and R. K. Hanson, in *Symposium (International) on Combustion*, 1998, vol. 27, pp. 95–101.
[25] R. Sur, K. Sun, J. B. Jeffries, and R. K. Hanson, *Appl. Phys. B*, vol. 115, no. 1, pp. 9–24, Jul. 2013.
[26] G. B. Rieker, J. B. Jeffries, and R. K. Hanson, *Appl. Opt.*, vol. 48, no. 29, pp. 5546–5560, Oct. 2009.
[27] L. S. Rothman, I. E. Gordon, Y. Babikov, A. Barbe, D. Chris Benner, P. F. Bernath, M. Birk, L. Bizzocchi, V. Boudon, L. R. Brown, A. Campargue, K. Chance, E. A. Cohen, L. H. Coudert, V. M. Devi, B. J. Drouin, A. Fayt, J.-M. Flaud, R. R. Gamache, J. J. Harrison, J.-M. Hartmann, C. Hill, J.

T. Hodges, D. Jacquemart, A. Jolly, J. Lamouroux, R. J. Le Roy, G. Li, D. A. Long, O. M. Lyulin, C. J. Mackie, S. T. Massie, S. Mikhailenko, H. S. P. Müller, O. V. Naumenko, A. V. Nikitin, J. Orphal, V. Perevalov, A. Perrin, E. R. Polovtseva, C. Richard, M. A. H. Smith, E. Starikova, K. Sung, S. Tashkun, J. Tennyson, G. C. Toon, V. G. Tyuterev, and G. Wagner, *J. Quant. Spectrosc. Radiat. Transf.*, vol. 130, pp. 4–50, Nov. 2013.

[28] S. S. Penner, *Quantitative molecular spectroscopy and gas emissivities*. Addison-Wesley Pub. Co., 1959.